ELSEVIER
Materials Science and Engineering B63 (1999) 36–43
MATERIALS SCIENCE & ENGINEERING B
www.elsevier.com/locate/mseb

Superconducting cuprates and magnetoresistive manganites: similarities and contrasts

T. Venkatesan [a,*], R.P. Sharma [a], Y.G. Zhao [a,f], Z.Y. Chen [a], C.H. Lee [a], W.L. Cao [a], J.J. Li [a], H.D. Drew [a], S.B. Ogale [b], R. Ramesh [b], M. Rajeswari [b], T. Wu [a], I. Jin [a], S. Choopun [a], M. Johnson [c], W.K. Chu [d], G. Baskaran [e]

[a] *Department of Physics and Electrical Engineering, University of Maryland, College Park MD 20742, USA*
[b] *Materials and Nuclear Engineering Department, University of Maryland, College Park MD 20742, USA*
[c] *Naval Research Laboratories, USA*
[d] *Texas Center for Superconductivity, University of Houston, Houston TX, USA*
[e] *Institute for Mathematical Sciences, Taramani, Chennai, India*
[f] *Department of Physics, Tsinghua University, Beijing, China*

Abstract

We report on three different experiments on high temperature superconducting (HTS) cuprates and colossal magnetoresistive (CMR) manganites, which clearly bring out some of the important similarities and differences between the two material systems. The experiments involve the measurement of temperature dependence of the mean squared displacement of Cu and Mn ions from their equilibrium site in the case of the cuprates and the manganites, respectively, and their correlation with the transport property. In both cases the key ions in the materials (Cu for HTS and Mn for CMR) exhibit vibration amplitudes larger than that of ions in simple Debye solids and clearly show discontinuities in the vibration amplitudes as a function of temperature close to the phase transition temperatures. These point to the unequivocal participation of phonons in the transport processes and possibly in the onset of the phase transitions (i.e. superconductivity and ferromagnetism). The second set of experiments, involves femtosecond optical excitation of micro-strip resistors made of cuprates or manganites, and the subsequent measurement of the changes in the impedance on a 20 ps time scale. In the case of the manganites one measures the time scales involved in the ionization and reformation of a Jahn–Teller polaron and also the decay times of magnon excitors. In the case of the cuprates one sees a highly efficient pair breaking process with a very sharp resonance, with a width of only 100 meV, which is indicative of the role of a large intermediate excitation in the mechanism of high temperature superconductivity. In the third experiment, spin-polarized electrons injected from a manganite electrode into a superconductor are observed to break pairs at a rate far larger than unpolarized electrons. This effect seems very orientation dependent for the case of YBCO, which may shed new light on the transport of quasi-particles at YBCO interfaces.

Keywords: High temperature superconducting (HTS) cuprates; Colossal magnetoresistive (CMR) manganites; Cu and Mn ions

1. Introduction

Since the end of 1986, when high temperature superconductors came into being, the subject has captured the interest of one of the largest segment of the research community in any sub-field of Physics [1–5]. Despite the level and pace of the research, the origin of the nature of transport in the cuprates is still known piece meal and the microscopic mechanism of the pairing process still eludes us [6–9]. Even the normal state transport properties continue to challenge our understanding and truly innovative experiments are needed to get at the root of these issues [10–12]. Over the last 5 years or so the condensed matter community has been pursuing yet another family of perovskites, the colossal magnetoresistive manganites, with a degree of intensity second only to the high T_c cuprates [13,14]. This is simply because the underlying physics behind the observed phenomena, encompass some of the most exciting ideas in condensed matter Physics involving highly correlated electronic systems with strong electron–phonon coupling and magnetic interactions [15–18]. In

* Corresponding author.

0921-5107/99/$ - see front matter
PII: S0921-5107(99)00049-5

addition, familiar ideas in solid state chemistry involving electronic orbitals and bond hybridization have been readily adopted in this field [19,20]. The manganite system may be an enabler in furthering our understanding of the cuprates. In this system, the strong electron–phonon interaction results in a precisely and relatively easily measurable correlation of transport properties with lattice distortions from which lessons may be drawn regarding similar effects in the case of the cuprates. The more visible role of electron spins on the transport properties of the manganites may shed light on the role of antiferromagnetic order in the Cooper pairing mechanism in the cuprates. In this paper we present three different experiments involving both the cuprates and the manganites, which we believe are very important for furthering our understanding of these rather enigmatic materials systems.

2. Ion channeling study of ion dynamics

Let us consider some of the important similarities between the cuprates and the manganites. In the less conducting state of the materials the electrical transport can be understood as due to charge hopping between adjacent Cu or Mn sites. The hopping frequencies increase as the conductivity of the material increases and this has effects on the dynamic lattice distortions whose frequencies are comparable with phonon frequencies. Thus the lattice distortions would no longer follow the charge hopping when the system becomes very metallic and the hopping times become very fast. The role of lattice distortions and their impact on transport properties arises from an important similarity between the Cu^{2+} and Mn^{3+} ions which are both Jahn–Teller ions [21] and would strongly favor lattice distortions to reduce the electronic degeneracies of the valence electrons. Let us now take the case of the manganites and the cuprates one by one.

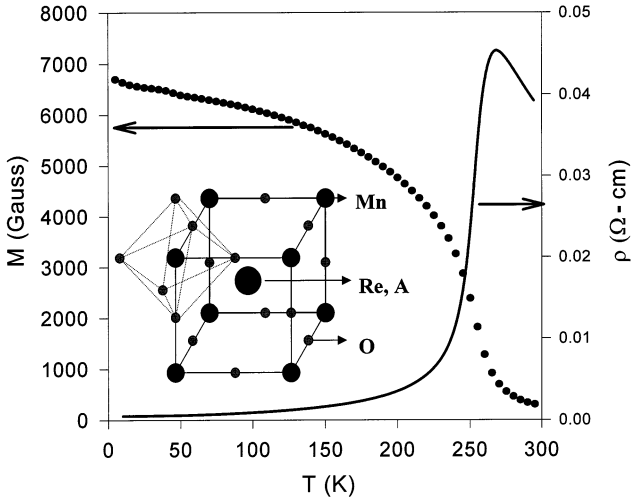

Fig. 1. Resistance vs. temperature curve for a film of $La_{0.7}Ca_{0.3}Mn_{0.3}$ film deposited by pulsed laser deposition. In the inset is shown the perovskite crystal structure of the manganite.

The manganites, characterized by the formula $R_{x-1}M_xMnO_3$ (where R = a trivalent rare earth ion such as La, Nd, Pr etc. and M = a divalent ion such as Ca, Ba, Sr), for the case of $x = 1/3$, can be represented by the transport property described by Fig. 1 [22,23]. In this case of $La_{0.7}Ca_{0.3}MnO_3$, the resistivity vs. temperature curve shows a bell shaped curve with the resistance exhibiting a peak close to the Curie temperature (270 K), so that above this peak the material is a paramagnetic semiconductor [24] and below this peak it is a ferromagnetic metal as evidenced by the onset of magnetization. The unique transport properties of this compound is understood as due to the hopping of an electron from a Mn^{3+} ion to an adjacent Mn^{4+} ion, via an intermediate oxygen atom. In this process the electron from the Mn^{3+} exchanges position with an electron in the $2p$ orbital of the oxygen and the original oxygen electron jumps concurrently into the Mn^{4+} valence level. In this 'double exchange' process [25], the strong Hund's rule coupling of the valence electrons to the core electrons, imposes a condition that the transition probability of the electron is proportional to the overlap of the spins at the two Mn core levels. The unusually large magnetoresistance and the ferromagnetic transition can be understood to some extent based on this double exchange idea. However, the observation of metallic behavior in this system at large resistivity values requires other mechanisms for charge localization and the Jahn–Teller distortion of the Mn–O–Mn bond is one such mechanism [26]. The Mn^{3+}–O and the Mn^{4+}–O bonds are not symmetric and the resultant distortion localizes the charge thereby raising the resistivity values. One of the important consequences of this idea is that when the electron hops from one Mn^{3+} to the next Mn^{4+}, it will be followed by a renormalization of the Mn–O bond configuration, provided the hopping times are comparable with phonon frequencies, which is true in the paramagnetic semiconducting state. However, as one gets into the metallic state where the hopping times become faster than the phonon response times, this effect becomes progressively weaker. Another way of looking at this is to say that in the semiconducting state the transport is via a small polaron whose size becomes progressively large as the metallicity increases with the electron becoming eventually itinerant as in conventional metals. So if the atomic displacements could be measured in these materials with a precision of better than 10^{-10} cm, then one ought to see dynamic displacements of the Cu or Mn ions in excess of the thermal vibrations expected for a Debye solid. One experimental technique that measures such displacements accurately is ion channeling spectrometry [27], though in the case of the manganites the

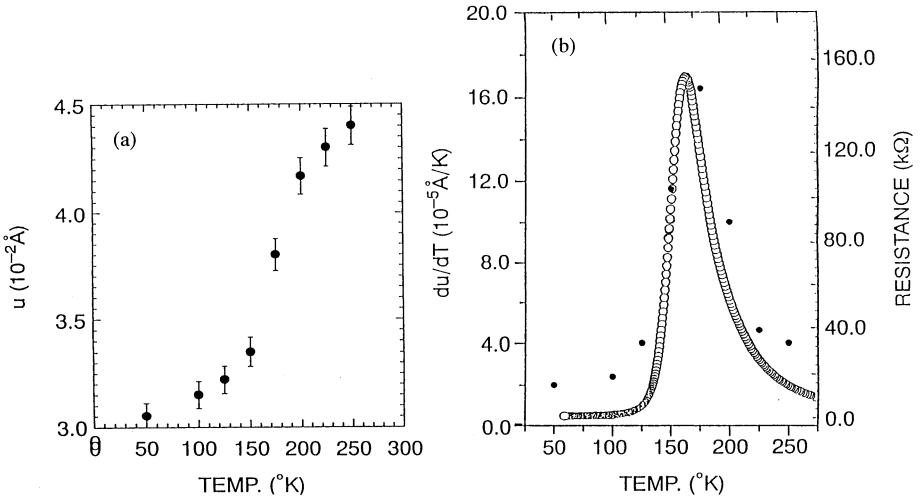

Fig. 2. (a) The displacement u of the Mn atoms from their equilibrium lattice positions as measured by ion channeling as a function of temperature in a 2000 Å thick film of $Nd_{0.7}Sr_{0.3}Mn_{0.3}$ grown on $LaAlO_3$ substrate. (b) The resistance vs. temperature curve for the manganites and the temperature derivative of the lattice displacement (u) [32].

effect is so large that even neutron scattering is able to measure such displacements unambiguously. However, in the case of the cuprates neutron scattering has not been as successful as ion channeling [28,29]. Details of the ion channeling technique can be obtained from a variety of references [30,31] and for brevity we will only deal here with the results of the measurements.

2.1. Ion channeling in the manganites

In Fig. 2 is shown the dynamic displacements measured for the compound $Nd_{0.7}Sr_{0.3}MnO_3$ by ion channeling technique in comparison with what is expected for a Debye solid [32]. Interestingly, in the paramagnetic state ($T > 170$ K) there are excess dynamic lattice distortions by as much as 50% of the thermal vibrations which vanish as one goes below the ferromagnetic transition (~ 170 K). In Fig. 3 is shown similar data for $La_{1.2}Sr_{1.8}Mn_2O_7$ a bilayer manganite system (an analog of YBCO, a Cu bilayer superconductor) and here again, the channeling data shows excess distortions in the system above the Debye values which then vanish below the Curie temperature (~ 100 K) progressively as the system becomes more metallic [33,34]. In some sense we could make a general remark that a system that has polaronic transport would at an insulator to metal transition show significantly larger vibration amplitudes than in a Debye solid and in the metallic state this excess distortion must vanish. Hence at a metal–insulator or normal metal–superconductor transition in a polaronic conductor one would expect to see dramatic changes in the excess lattice distortions.

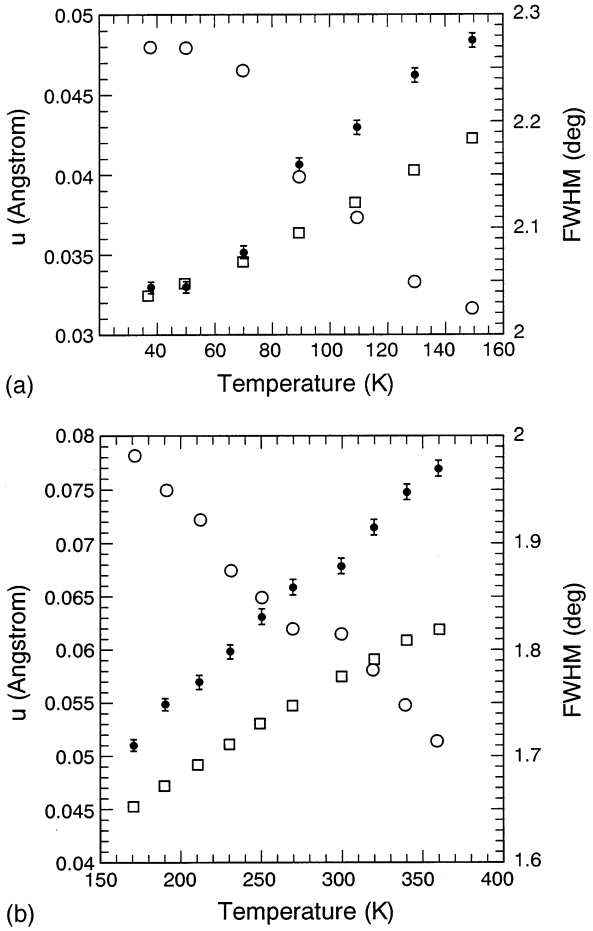

Fig. 3. (a) The displacements of the Mn atoms from their equilibrium lattice positions as measured by ion channeling as a function of temperature for a bilayer manganite, $La_{1.2}Sr_{1.8}Mn_2O_7$ in the temperature range of 36–150 K, the circles represent the FWHM of the channeling angular scans. (b) The same in the temperature range of 150–350 K [33,34].

2.2. Ion channeling in the cuprates

In Fig. 4 is shown the channeling data for single crystal YBCO with the vibration amplitudes of Cu plotted for an oxygen deficient YBCO (non-superconducting) and a fully superconducting YBCO ($T_c = 92.5$ K) [35]. Also shown are the Debye curves for both the systems (with Debye temperatures $T = 330$ and 380 K for the non-superconducting and superconducting samples). The non-superconducting YBCO shows a monotonic behavior while the superconducting sample shows a variety of unusual discontinuities with temperature. The fact that the non-superconducting sample shows a larger vibration amplitude, and that the superconducting sample shows a drop in this vibration amplitude abruptly at the transition temperature is proof that there is a dramatic difference in the role of phonons in the transport properties above and below T_c. If we took the analogy from the manganites one would say that the system has evolved from a polaronic behavior above T_c to some thing less polaronic below the T_c. While the polaron in the case of the manganite arises because of the difference in the Mn–O bond configuration depending on the valence state of the Mn, in the case of the cuprates the polaron may arise from a different origin. Since the Cu valences are believed to be predominantly $2+$ in the superconducting phase, the argument arises as to where the hole responsible for transport resides. Energetics arguments preclude the hole from being localized either on the Cu or the O atom. Molecular entities such as Zhang–Rice singlets (ZRS) [36], where the hole is shared by a square of four oxygen atoms with the spin of the Cu electron and that of the hole forming a singlet seem highly plausible. If such molecular entities facilitate the hopping of charge from site to site, then the Cu–O bond configuration of the ZRS would be affected by the hole occupancy of the site. Thus by arguments similar to the case of the manganites one would expect an ion channeling signature in the less conductive state of the material as is indeed seen. Further, in the superconducting state, where the electrons become truly itinerant the excess vibrations die down completely. What is indeed remarkable is that even at 90 K, the system already reaches the zero-point vibration of the system suggesting a coherent state for the ionic sites as well! The freezing of the Cu motion has been further verified recently by EXAFS technique [37]. The unusual transitions seen at 150, 200 K and at higher temperatures show the possibility of other phonon mediated behavior in the system, not obvious in the transport measurements which would require further exploration.

In summary, ion channeling experiments with ability to measure small vibration amplitude of the atoms from their equilibrium positions may be a very valuable tool for understanding the transport properties of the perovskite based conductors where strong electron–phonon effects are seen in addition to strong electron correlation.

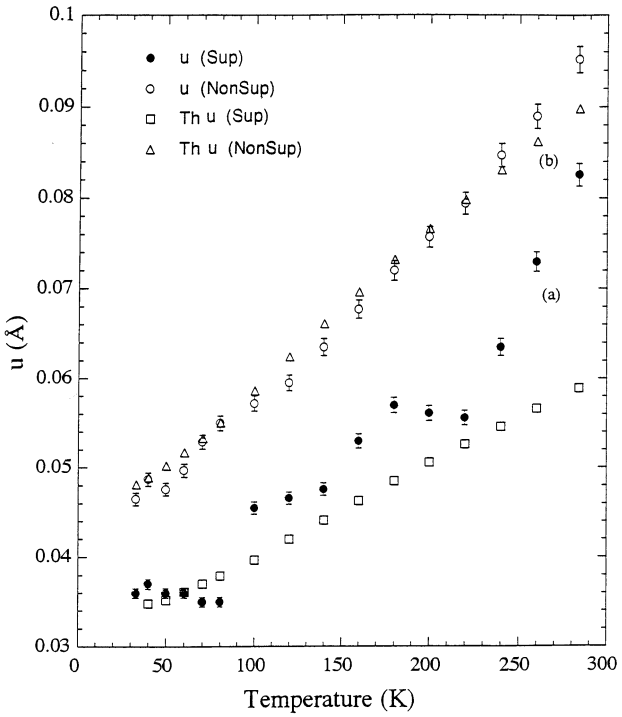

Fig. 4. Displacements of the Cu atom in the case $YBa_2Cu_3O_{7-\delta}$ superconductor as measured by ion channeling as a function of temperature for $\delta = 0.77$ (non-superconducting) and $\delta = 0.05$ (superconducting) samples. In the non-superconducting case the Debye fit (triangles) with a Debye temperature of 330 K, and in the superconducting case the Debye fit (squares) with a Debye temperature of 380 K is shown [31].

3. Optical excitation study of electron dynamics

We can learn significant information about the material systems by studying their electron dynamics. In retrospect the previous section dealt with dynamics of the ions measured by a technique which takes snap shots of the nuclei at very short time intervals ($\sim 10^{-20}$ s determined by the ion scattering times)[1]. Now we want to focus on the electron dynamics. In the following technique we use 100 fs laser pulses to excite the electrons in the system and see the rise and decay times

[1] The Ion Scattering time depends on the distance of closest approach or the impact parameter which is of the order of a few Fermi and depends on the atomic number of the incident ion and the target nucleus. Since the velocity of the incident ion is $\sim 10^9$ cm per s, these times are in the range of 10^{-19}–10^{-21} s.

at different temperatures where the property of the material changes. The experiment consists of measuring the changes in the impedence of a transmission line built out of the material of interest. While readers can get details elsewhere [38], the measurement times are essentially limited by the oscilloscope rise time, which is 20 ps, as a result of which processes faster than 20 ps will be averaged in this time scale. Once again, let us consider the case of the manganites first since the data

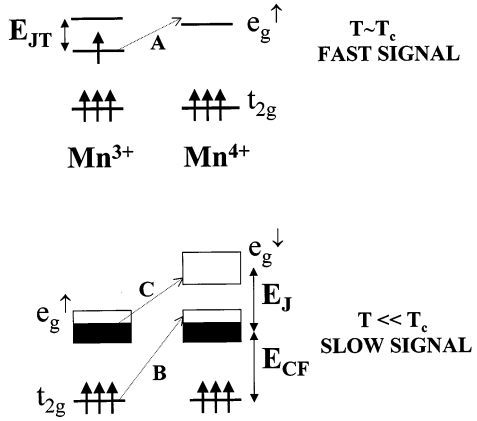

Fig. 5. The electronic energy levels and the possible optical transitions in the paramagnetic and ferromagnetic states of the manganites [41].

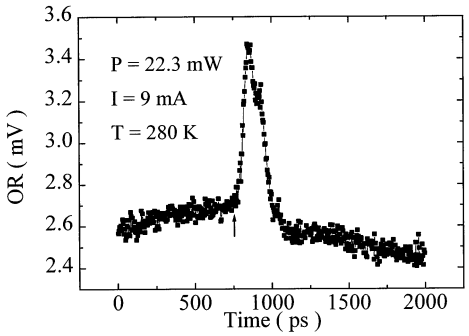

Fig. 6. Optical response consisting of a photoconductivity signal at a temperature of 280 K, close to the ferromagnetic transition temperature in the case of $La_{0.7}Ca_{0.3}MnO_3$ (LCMO) film [41].

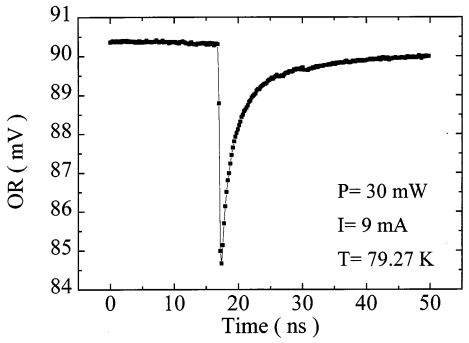

Fig. 7. Optical response consisting of a photoresistive transient at a temperature of 79.27 K, where the LCMO is in the fully ferromagnetic state [41].

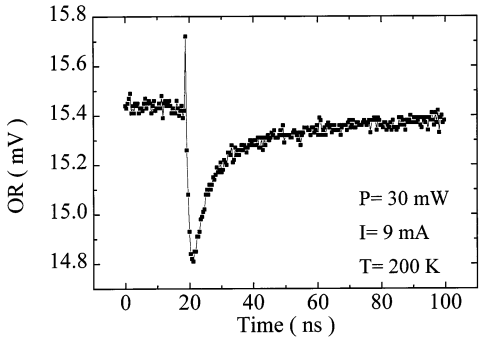

Fig. 8. Optical response at an intermediate temperature of 200 K for LCMO where both the conductive and resistive transients are seen [41].

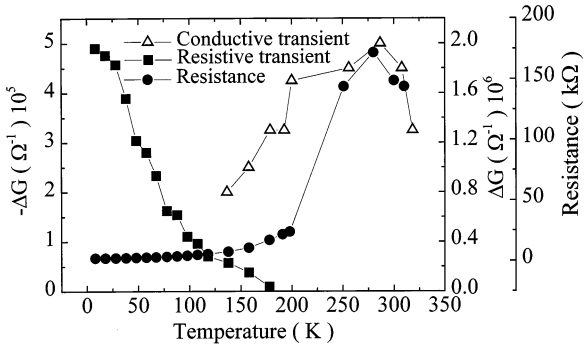

Fig. 9. The behavior of the resistive and conductive transients with respect to temperature and comparison with the resistance curve [41].

is relatively easier to interpret. At temperatures close to the Curie temperature where the system has Jahn–Teller splitting, the energy levels for the electronic transition can be considered as shown in Fig. 5 [39,40]. For the 1.5 eV photon the most likely transition is that of an electron from the lower e_g orbital of the Mn^{3+} to the e_g orbital of the Mn^{4+} ion (Transition A) [41]. This essentially ionizes the polaron, which will increase the conductivity and indeed such a signal is seen as shown in Fig. 6. The rise time of the conductivity transient signal is of the order of 40–60 ps and the fall time is of the order of 150 ps. It is not clear at this point as to what these times signify. Besides the Jahn–Teller distortion arising from the Mn^{3+} ion, the Mn^{4+} ions exhibit an oxygen-breathing mode distortion which also causes changes in the electronic energy levels promoting localization. So when the electron is promoted from the Mn^{3+} to the Mn^{4+} ion the Jahn–Teller and the breathing mode distortions must change sites effectively. Since the hopping ti2mes close to the ferromagnetic transitions are likely to be slow one ought to see polaronic effects accompanying charge transfer. The fall time represents the trapping time for the excited electron or the reformation time for the Jahn–Teller polaron. At very low temperatures where the system becomes a good ferromagnetic metal the signal has opposite behavior; it is a resistive transient and is

significantly slower (Fig. 7). Based on the slow response and resistance increase, this signal is interpreted as due to magnon formation and its recombination. This time comes out to be of the order of tens of nanoseconds and is also very temperature dependent with the time constant becoming longer with increasing temperature. Transition B in Fig. 5, the most resonant, would produce a spin flip excitation with some help from the weak spin orbit coupling in the system, and the relaxation will be via magnon decay. The magnon decay times are an order of magnitude larger than those for conventional metallic magnetic systems such as Ni [42–44], which is consistent with the order of magnitude narrower resonance line width measured in the manganites by ferromagnetic resonance experiments [45]. (What is still not resolved is the strength of the transition B which seems comparable with that of A, though the former should be weak on account of the small spin orbit coupling in the manganite system). At intermediate temperatures one observes both the conductive and resistive components

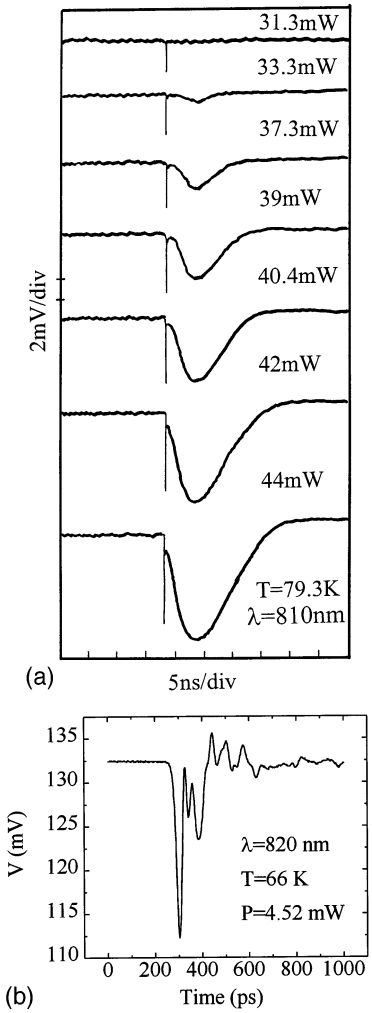

Fig. 10. (a) The fast and slow optical response observed under fs. laser excitation of the superconductor. (b) The fast response on an expanded time scale [38,50]

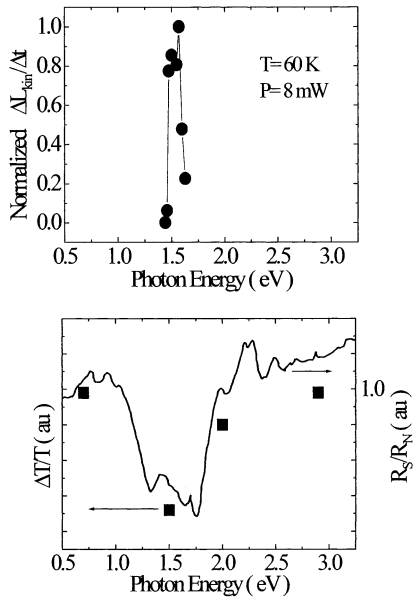

Fig. 11. The Optical response (proportional to the Cooper pair breaking rate) vs. excitation energy of the photon for YBCO (upper panel), compared with the data from Refs. [46] (solid line) and [47] (solid squares) as shown in lower panel [50].

(Fig. 8) which tells us that the evolution of the system from a paramagnetic semiconductor to a ferromagnetic metal is a gradual evolution and as shown in Fig. 9 the system crosses over at temperatures below $T_c/2$ from a predominantly paramagnetic behavior to a ferromagnetic behavior. The system evolves from an ionic bond picture to an itinerant metallic band picture!

Let us look at the case of the cuprates now. What one sees at a given photon energy is a two component excitation (Fig. 10a) where the slow component has been clearly identified as due to thermal effect while the fast initial component (Fig. 10b) is interpreted as a kinetic inductance change arising from pair breaking effects [38]. The photon dependence of this fast component (Fig. 11) is quite exciting since one sees a resonance centered at about 1.53 eV with a FWHM of only 100 meV. This is indeed an unusual result in the sense that such a narrow excitation is possible at all in such a strongly correlated electronic system in the superconducting state. Two different observations [46,47] prior to this have confirmed the existence of a resonance around 1.5 eV in the case of the cuprates, but neither of them involved direct pair breaking. Instead they were measurements of index changes and had much broader features ($\sim$500 meV) as seen in Fig. 11. While the intrinsic processes of excitation and decay are much faster than our measurement times of 20 ps, the optical resonance is qualitatively correct and identifies a high-energy excitation responsible for the pair breaking, in consistence with the observation of [46,47]. Taking the analogy of the manganites if one considers this as an ionization of a ZRS (whose separation from the upper

Hubbard band has been identified via photoemission experiments [48,49] to be around 1.4 eV), then the pair breaking could be consistently explained [50]. Thus the optical excitation experiment further supports the findings from the channeling results.

4. Spin-polarized quasi-particle injection into high temperature superconductors

In the last set of experiments, we have coupled the HTS and CMR together to study the effect of spin-polarized electrons on the superconductor. All the efforts in this direction to date [51–53] consist of FET structures in which the critical current of the HTS channel is modulated by spin-polarized current injected from a CMR gate electrode. This modulation is compared with the gate electrode replaced by a non-ferromagnetic electrode such as Lanthanum nickel oxide, which is structurally and thermodynamically very similar to the manganites. When the gate current is injected along the c-axis with the super current flowing in the a–b plane, the spin-polarized electrons are effective at breaking Cooper pairs at least a factor of 15–30 times larger than unpolarized electrons (Fig. 12) [52]. When such an experiment is performed for the case where the channel is replaced by an a-axis oriented YBCO film, with gate current along the a-axis and the super current along the huxis in the b–c plane, the difference between the spin-polarized and unpolarized pair breaking efficiency becomes much smaller. This result has significant impact on some of the current theoretical description of charge transport in the cuprates. Anderson [54] has postulated that in the case of the cuprates it may be easier to transport a paired electron along the c-axis as opposed to a single quasi-particle. From a ferromagnetic electrode it will be difficult to produce a singlet pair of electrons and any alternative would enable better pair breaking than the case where the electrons are injected as correlated pairs as can happen from a non-ferromagnetic gate electrode. However, there are still some unresolved issues relating to thermal effects in these experiments which need to be put to rest before the results can be fully considered. The connections with the previous two experiments is as follows. The concept of the unusual pair transport along the c-axis of cuprates applies to the system where spin-charge separation exists. ZRS will manifest spin-charge separation and thus the spin-polarized quasi-particle pair breaking data may be an indirect proof of YBCO being a system in which spin-charge separation exists [12].

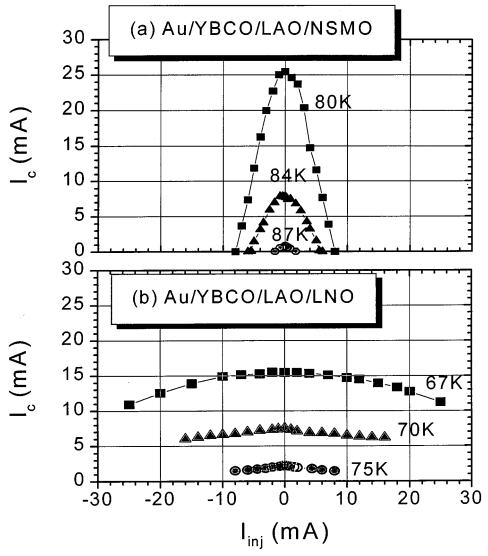

Fig. 12. Critical Current vs. gate injection current at different temperatures for: (a) ferromagnetic manganite ($Nd_{0.7}Sr_{0.3}MnO_3$) gate injector and (b) non-ferromagnetic metallic gate injector ($LaNiO_3$).

5. Summary

These three sets of experiments, which probe ion, electron and spin dynamics, need to be refined further, though even at this stage the data produced by these experiments clearly point to exciting ways for us to unravel the mystery of these materials. The rejuvenation of research in the manganite is certainly having a synergistic effect on the cuprate research.

Acknowledgements

The authors would like to acknowledge ONR Grant No. ONR-N000149611026 (Program Monitor: Deborah Van Vechten) and NSF MRSEC Grant No. DMR96-32521. T. Venkatesan would like to thank the Institute of Mathematical Sciences, Chennai (Madras), India for their hospitality, during a portion of this work.

References

[1] J.G. Bednorz, K.A. Muller, Z. Phys. B64 (1986) 189.
[2] Proceedings of the 19th International conference on low temperature physics, Physica B, 165–166 (1990).
[3] Proceedings of the International conference on Materials and Mechanisms of Superconductivity, M. Tachiki, Y. Muto, Y. Syono (Eds.), High Temperature Superconductors III, Kanazawa, Japan (1991).
[4] Proceedings of the 1996 Applied Superconductivity Conference, IEEE Trans. Appl. Supercond., Vol. 7 (1997)
[5] Proceedings of the 21st International Conference on Low Temperature Physics, Czechoslov. J. Phys. 4 Suppl. (1996).
[6] D. Pines, P. Monthoux, J. Phys. Chem. Solids 56 (1995) 1651.
[7] D.J. Scalpino, J. Phys. Chem. Solids 56 (1995) 1669.
[8] P.J. Hirschfeld, W.O. Putikka, D.J. Scalapino, Phys. Rev. B50 (1994) 10250.

[9] P.J. Hirschfeld, W.O. Putikka, D.J. Scalapino, Phys. Rev. Lett. 71 (1993) 3705.
[10] P.W. Anderson, Science 235 (1987) 1196.
[11] P.W. Anderson, G. Baskaran, Z. Zou, T. Hsu, Phys. Rev. Lett. 58 (1987) 2790.
[12] Q. Si, Phys. Rev. Lett. 78 (1997) 1767.
[13] Proceedings of Telluride Summer Research Center workshop on Magnetoresistive Oxides, Telluride, Collorado (1998).
[14] Proceedings of Mat. Res. Soc. Symp. CMR materials, Boston (1997).
[15] A.J. Millis, P.B. Littlewood, B.I. Shraiman, Phys. Rev. Lett. 74 (1995) 5144.
[16] N. Furukawa, J. Phys. Soc. Jpn. 64 (1995) 2754.
[17] N. Furukawa, J. Phys. Soc. Jpn. 64 (1995) 2734.
[18] N. Furukawa, J. Phys. Soc. Jpn. 65 (1996) 1174.
[19] J.B. Goodenough, Phys. Rev. 100 (1955) 564.
[20] J. Toepfer, J.B. Goodenough, J. Solid. State. Chem. 130 (1997) 117.
[21] C. Kittel, Introduction to Solid State Physics, John Wiley and Sons, New York, 1986.
[22] G.C. Xiong, Q. Li, H.L. Ju, S.N. Mao, L. Senapati, X.X. Xi, R.L. Greene, T. Venkatesan, J.M. Byers, M. Rubinstein, Appl. Phys. Lett. 66 (1995) 1427.
[23] G.C. Xiong, Q. Li, H.L. Ju, S.N. Mao, L. Senapati, X.X. Xi, R.L. Greene, T. Venkatesan, J.M. Byers, M. Rubinstein, Appl. Phys. Lett. 66 (1995) 13.
[24] G.C. Xiong, S.M. Bhagat, Q. Li, M. Dominguez, H.L. Ju, R.L. Greene, T. Venkatesan, J.M. Byers, M. Rubinstein, Solid State Comm. 97 (1996) 599.
[25] C. Zener, Phys. Rev. 82 (1951) 403.
[26] A.J. Millis, P.B. Littlewood, B.I. Shraiman, Phys. Rev. Lett. 77 (1996) 175.
[27] L.C. Feldman, J.W. Mayer, S.T. Picraux, Materials Analysis by Ion Channeling, Academic Press, 1982.
[28] R.P. Sharma, F.J. Rotella, J.D. Jorgensen, L.E. Rehn, Physica C174 (1991) 409.
[29] P. Schweiss, W. Reichardt, M. garden, G. Collin, G. Heger, H. Claus, A. Erb, Phys. Rev. B49 (1994) 1387.
[30] R.P. Sharma, L.E. Rehn, Studies of High Temperature Superconductors Advances in Research and Applications, in: Anant Narlikar (Ed.), Nova Science Publishers, vol. 15, 1995, pp. 1–48.
[31] R.P. Sharma, T. Venkatesan, Z.H. Zhang, J.R. Liu, R. Chu, W.K. Chu, Phys. Rev. Lett. 77 (1996) 4624.
[32] R.P. Sharma, G.C. Xiong, C. Kwon, R. Ramesh, R.L. Greene, T. Venkatesan, Phys. Rev. B54 (1996) 10014.
[33] R.P. Sharma, P. Fournier, R.L. Greene, T. Venkatesan, J.F. Mitchell, D. Miller, J. Appl. Phys. 83 (1998) 7351.
[34] R.P. Sharma. P. Fournier, M. Downes, S. Choopun, R.L. Greene, T. Venkatesan, J.F. Mitchell, D. Miller, T. Kimura, Y. Tokura, unpublished.
[35] R.P. Sharma, T. Venkatesan, Z.H. Zhang, J.R. Liu, R. Chu, W.K. Chu, B. Veal, A Paulikas, H. Zheng, unpublished.
[36] F.C. Zhang, T.M. Rice, Phys. Rev. B37 (1988) 3759.
[37] J. Röhler, P.W. Loeffen, S. Müllender, K. Conder, E. Kaldis, Proceedings of the NATO ASI on Materials Aspect of High T_c Superconductors, in: E. Kaldis, et al. (Eds.), Kluwer Academic, 1997, p. 469.
[38] Y.G. Zhao, S.B. Ogale, R. Shreekala, Z.W. Dong, S.P. Pai, M. Rajeswari, T. Venkatesan, W.L. Cao, W. Lu, C. Lee, J. Appl. Phys. 83 (1998) 1531.
[39] J.M.D. Coey, M. Virt, R.K. Ounadjela, Phys. Rev. Lett. 75 (1995) 3910.
[40] S. Kaplan, M. Quijada, H.D. Drew, D.B. Tanner, G.C. Xiong, R. Ramesh, M. Rajeswari, T. Venkatesan, Phys. Rev. Lett. 77 (1996) 2081.
[41] Y.G. Zhao, J.J. Li, R. Shreekala, H.D. Drew, C.L. Chen, W.L. Cao, C.H. Lee, M. Rajeswari, S.B. Ogale, R. Ramesh, G. Baskaran, T. Venkatesan, Phys. Rev. Lett. 81 (1998) 1310.
[42] E. Beaurepaire, J.C. Merle, A. Daunois, J.Y. Bigot, Phys. Rev. Lett. 76 (1996) 4250.
[43] A. Scholl, L. Baumgarten, R. Jacquemin, W. Eberhardt, Phys. Rev. Lett. 79 (1997) 5146.
[44] M. Aeschlimann, M. Bauer, S. Pawlik, W. Weber, R. Byrgermeister, D. Oberli, H.C. Siegmann, Phys. Rev. Lett. 79 (1997) 5158.
[45] M.C. Robson, C. Kwon, K.C. Kim, R.P. Sharma, R. Ramesh, T. Venkatesan, S.E. Lofland, M. Domingue, S.D. Tyagi, S.M. Bhagat, J. Appl. Phys. 80 (1996) 2334.
[46] M.J. Holcomb, C.L. Perry, J.P. Collman, W.A. Little, Phys. Rev. B53 (1996) 6734.
[47] C.J. Stevens, D. Smith, C. Chen, J.F. Ryan, B. Podobnik, D. Mihailovic, G.A. Wagner, J.E. Evetts, Phys. Rev. Lett. 78 (1997) 2212.
[48] M. Mertz, N. Nucker, E. Pellegrin, P. Schweiss, S. Schuppler, M. Kielwein, M. Knupfer, M.S. Golden, J. Fink, C.T. Chen, V. Chakarian, Y.U. Idzerda, A. Erb, Phys. Rev. B55 (1997) 9160.
[49] M. Mertz, N. Nucker, P. Schweiss, S. Schuppler, C.T. Chen, V. Chakarian, J. Freeland, Y.U. Idzerda, M. Klasre, G. Muller-Vogt, Th. Wolf, Phys. Rev. Lett. 80 (1998) 5192.
[50] Y.G. Zhao, W.L. Cao, J.J. Li, R. Shreekala, C.H. Lee, H.D. Drew, S.P. Pai, M. Rajeswari, S.B. Ogale, G. Baskaran, T. Venkatesan, unpublished.
[51] V.A. Vas'ko, V.A. Larkin, P.A. Kraus, K.R. Nikolaev, D.E. Grupp, C.A. Nordman, A.M. Goldman, Phys. Rev. Lett. 78 (1997) 1134.
[52] Z.W. Dong, R. Ramesh, T. Venkatesan, M. Johnson, Z.Y. Chen, S.P. Pai, V. Talyansky, R.P. Sharma, R. Shreekala, C.J. Lobb, R.L. Greene, Appl. Phys. Lett. 71 (1997) 1718.
[53] R.J. Soulen, M.S. Osofsky, D.B. Chrisey, J.S. Horwitz, D. Coller, R.M. Stroud, J. Kim, C.R. Eddy, J.M. Byers, B.F. Woodfield, G.M. Daly, T.W. Clinton, M. Johnson, R.C.Y. Auyeung, Appl. Supercond. 1–2 (158) (1997) 789.
[54] P.W. Anderson, The Theory of High Temperature Superconductivity, Princeton University Press, Princeton, USA, 1997.